Ordered Polyelectrolyte "Multilayers". 5. Photo-Cross-Linking of Hybrid Films Containing an Unsaturated and Hydrophobized Poly(diallylammonium) Salt and Exfoliated Clay

Pascal Y. Vuillaume,‡ Alain M. Jonas,‡ and André Laschewsky*,†,§

Département de Chimie, Université Catholique de Louvain, Place L. Pasteur, 1, B-1348 Louvain-la-Neuve, Belgium; and Unité de Physique et de Chimie des Hauts Polymères, Université Catholique de Louvain, Place Croix du Sud, 1, B-1348 Louvain-la-Neuve, Belgium

Received December 3, 2001; Revised Manuscript Received March 25, 2002

ABSTRACT: A simple synthetic route to a new poly(diallylammonium) salt functionalized by a styrene group is presented. This reactive polymer was employed for polyelectrolyte multilayer films using electrostatical layer-by-layer self-assembly, together with an inorganic polyanion, namely an exfoliated hectorite clay. To enhance their stability, the final hybrid multilayers were cross-linked by exposure to UV light, leading only to a minor shrinkage. Alternatively, the reactive polycation was cross-linked after each adsorption step. X-ray reflectometry revealed that the two types of films dispose of an internal order with a short length scale, that seems insensitive to the photo-cross-linking. Cross-linking after each adsorption step, however, results in more regular film growth, and reduces the films' roughness and the amount of polyanion deposited. Under these conditions, the films seem to grow by deposition of submonolayers with a combined vertical and lateral expansion, resulting in the self-healing of previously deposited, incomplete layers.

Introduction

Over the past decade, the scope of the electrostatic self-assembly (ESA) technique has been intensely studied due to its simplicity and versatility.[1,2] Under appropriate conditions, polyelectrolytes may be deposited layer-by-layer on a charged substrate, by immersing a substrate successively in solutions containing complementary charged polyelectrolytes. A wide range of charged entities can be used with this method, leading to complex assemblies of controlled thickness with numerous functionalities. Internal order within such films may be an important aspect for practical applications. However, concerning the fabrication of ordered organic thin films, little progress has been made so far.[2] Although it was demonstrated recently that internally ordered assemblies can be obtained by ESA from pure organic polyelectrolytes that exhibit lyotropic liquid crystalline behavior,[3,4a] such ordering is exceptional.[4a] The fabrication of well-ordered assemblies deserves therefore continuous attention, by virtue of the simplicity of the ESA process as such.[1,2,5] Recently, hybrid multilayered assemblies were reported that exhibit internal order, namely defined sublayers.[6−9] This was achieved by replacing one of the flexible polyelectrolytes by charged inorganic platelets, as obtained by the exfoliation of layered alumosilicate clays. But so far, the ESA technique applied to hybrid coatings could not produce assemblies with extended positional order,[6] and therefore, other strategies are explored in our laboratory to prepare ordered hybrid assemblies with a long range order.[10,11]

For a number of potential applications, the preservation of the structural integrity of supramolecular assemblies is crucial.[12] Despite the incorporation of alumosilicate sheets which can provide internal reinforcement and enhancement of mechanical properties,[13] hybrid ESA assemblies are hydrogels and thus must be considered as "soft" and sensitive materials, like purely organic polyelectrolytes thin films. For example, exposure to aggressive solvents, aging, and high temperature generally affect the dimensional and chemical integrity.[2a] Nevertheless, most of the attempts to stabilize self-assembled multilayers have been focused on Langmuir−Blodgett films,[14−17] whereas up to now, only few cross-linkable ESA systems have been investigated.[18−22] The approaches generally rely on the cross-linking reaction via a condensation reaction of complementary groups located on adjacent layers. For example, one finds three-dimensional network multilayers formed by condensation of polymeric amines (such as poly(ethylenimine) or poly(allylamine)) with bifunctional aldehydes for forming a Schiff base,[20] or with polymeric acids (such as poly(acrylic acid) or poly(amic acids)) leading to amide or imide bonds, respectively.[21] Diazoresins have been employed as well, as these photoreactive polycations can react with complementary anionic groups, such as carboxylates or sulfonates, to establish covalent bonds,[22] though this reaction may be not very efficient.[22g] However, these above strategies are not suited for hybrid systems where polyelectrolyte layers alternate with a charged inorganic clay. Cross-linking of hybrid layers was only reported by sol−gel chemistry of clays with tetraalkoxysilanes.[19] An alternative strategy would be the use of photo-cross-linkable polyelectrolytes,[18a] which to our knowledge has not been employed yet in hybrid assemblies.

We have recently tested a wide range of functional poly(diallylammonium) salts that could be self-assembled with a particular exfoliated synthetic hectorite, namely Laponite. Such systems are rather robust

* To whom correspondence should be addressed.
† Département de Chimie, Université Catholique de Louvain.
‡ Unité de Physique et de Chimie des Hauts Polymères, Université Catholique de Louvain.
§ Permanent address: Fraunhofer Institut für Angewandte Polymerforschung FhG-IAP, Geiselbergstrasse 69; D-14476 Golm, Germany.

10.1021/ma012095a CCC: $22.00
Published on Web 05/17/2002

for forming internal structure.[18b] Since the synthesis of poly(diallylammonium) derivatives is rather variable,[23−26] a new rigid unsaturated polycation based on poly(diallylammonium) backbone and its cross-linkable derivative was therefore designed. In addition to an enhanced stability of the films, the use of a cross-linkable polycation could promote the understanding of the film growth process. By freezing in the uppermost organic layer before the tiling process, we expect less reorganization of the polyelectrolytes during the film growth[1,2] in the films. Also, we wanted to study cross-linkable systems with respect to a possible limiting of the interdiffusion between platelets and polyelectrolytes. Speculatively, such a scenario could promote the internal ordering. From a practical point of view, this strategy may offer additional benefits such as the improvement of the barrier properties[12] and the control of the permeability between sublayers of the ESA films.[7b]

Experimental Section

Materials. All the solvents used were of analytical grade. Dimethylformamide (DMF, Riedel-de Haën), acetonitrile (Merck), and dimethyl sulfoxide (DMSO, Fluka) were dried over molecular sieves (4 Å). Dioxane (Acros Organics), *tert*-butyl alcohol (Janssen), 1,2,3,4-tetrahydroisoquinoline [Aldrich (97%)], potassium *tert*-butoxide [Fluka, (97%)], dinitrobenzene [(99%)], quinone [Aldrich, (99%)], phenothiazine [Janssen, (99%)], 2,2′-dimethyl-2,2′-azo-*N*-(2-hydroxyethyl)propionamide (VA086, gift from WAKO) were used as received. Allyl chloride [Acros, (99%)] was distilled over calcium chloride and dimethyl sulfate [Aldrich (97%)]. Potassium persulfate ($K_2S_2O_8$, Acros) was recrystallized from water. Column flash chromatography was performed using silica gel [Merck, Kieselgel 60 (230−400 mesh)] or basic alumina (Acros, activated basic, 50−200 μm). Thin-layer chromatography (TLC) was carried out on precoated silica gel (Kieselgel 60, Merck, F-254) or on alumina (aluminum oxide Kieselgel 60-F254). Dialysis membranes (Spectra/Por) had a nominal cutoff of 6000−8000 Da. Water used for dialysis and for multilayer build up was purified by a Elgastat Maxima system (resistance 18.2 MΩ). Laponite [anal. (%): SiO_2, 60; MgO, 29; Li_2O, 0.9; Na_2O, 2,9; 9.8 weight loss of ignition] from Laporte Industry was a gift from Chimilab Essor (La Madeleine, France).

Substrates and Multilayers Assemblies. Quartz plates (Suprasil) and one-side polished silicon wafers (100) [ACM, (France)] were used as substrates for the deposition of the charged entities. Quartz plates were first sonicated in cold ethanol and both type of substrates were cleaned for 1 h in a piranha mixture [H_2SO_4/H_2O_2 (30%) 1:3 (v/v)] [*Caution! "piranha solution" is extremely corrosive and reacts violently with organic compounds*], left at ambient temperature, and then thoroughly washed with pure water. Details relative to the preparation and the characterization of Laponite dispersions are given elsewhere.[6] Typical concentrations of the polyelectrolyte solutions are in the range 10^{-2}−10^{-3} mol·L^{-1} (based on repeat units). Syringe filters (PTFE, 0.45 μm, Alltech) served for filtering polyelectrolyte solutions and Laponite dispersions.

Assemblies were built up directly on the supports, without any precoating. The cross-linkable polycation **6** (see the chemical structure in Figure 1) was adsorbed from solutions in DMSO. Immersion times were 10 min each for the adsorption of Laponite and of the polycation. After each deposition of the cross-linkable polycation, the substrate was immersed successively in three beakers containing DMSO, DMSO/water (50/50 v/v) and pure water. Samples were washed thrice with pure water after deposition of Laponite to prevent any cross-contamination. Multilayers were polymerized by exposure to UV light (λ = 254 nm, nominal power of 8 W (Rayonet photochemical reactor lamp)) in air for 10 min at a 5 cm distance. Samples were exposed either after each deposition of cross-linkable polycation, or at the end of the multilayer build-up. Layer-by-layer cross-linked multilayers were dried for 2 min by hot air between successive deposition cycles, while un-cross-linked multilayers were dried with a stream of cold air for 8 min. UV measurements were carried out immediately after the self-assembly. Silicon wafers destined for X-ray investigations were stored in a dark and cool place. In the following, ESA assemblies will be presented in the form of {**A**,**B**}$_x$ describing a multilayer film made of x cycles of polycation **A** with polyanion **B**.

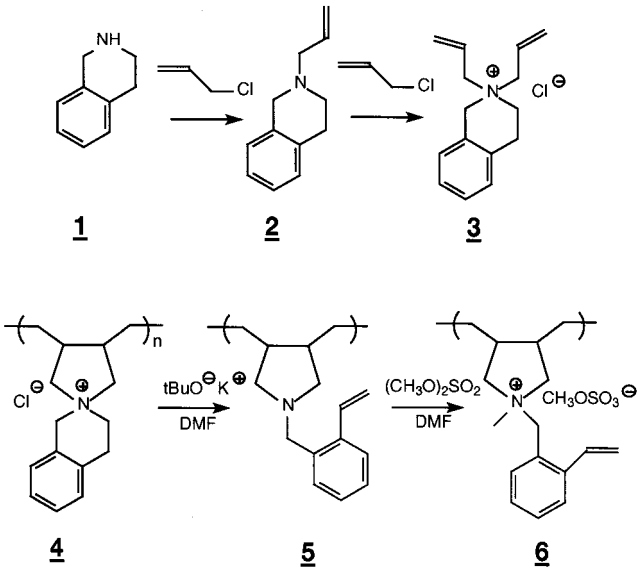

Figure 1. Synthetic route leading to monomer **3** and polymers **4**−**6.**

Methods. NMR spectra were recorded with Gemini 200 or 300 Varian spectrometers and with a Bruker 500 MHz. Chemical shifts, δ, are given in ppm with respect to the solvent residual resonances fixed at 7.27 ppm, 2.49 ppm, 4.80 ppm, 3.30 ppm for $CDCl_3$, $(CD_3)_2SO$, D_2O, and CD_3OD, respectively. Elemental analysis was done at the University College of London. Mass spectrometry was performed by the Mass Spectrometry Laboratory of the Université Catholique de Louvain, with a SCIEX API III triple quadruple mass spectrometer. FT-Infrared spectra were recorded in KBr pellets on a Bruker Equinox FTIR spectrometer. 256 scans with a resolution of 2 cm^{-1} were taken for each sample. UV−vis spectra were taken from films deposited on quartz plates with a Varian Carry SE spectrometer. The values of λ_{max} were determined at the maximum of the peak after smoothing the data by the Savitsky Golay algorithm. Thermogravimetric analysis was carried out under constant nitrogen flow (200 mL·min^{-1}) at a heating rate of 10 °C/min using a Mettler Toledo STAR^e system. The samples were previously dried in situ at 80 °C for 15 min just prior to the heating scans. Differential scanning calorimetry (DSC) was carried out on samples of about 11 mg sealed in aluminum pans with previously pierced covers using a Perkin-Elmer DSC-7, calibrated with indium and zinc. The polymers were dried for at least 2 days at 60 °C in vacuo and scanned with a heating rate of 10 °C/min [after both slow cooling (20 °C/min) and quenching (nominally 200 °C/min)]. Ellipsometry was performed on a Digisel rotating compensator ellipsometry from Jobin-Yvon/Sofie Instruments, at the wavelength of 6328 Å (He−Ne laser) and a fixed incidence angle of 70°. Each data point was averaged by performing two measurements with the analyzer successively set to +45 and −45° (with respect to the plane of incidence).[27] For each sample, at least eight different measurements at different positions were made and averaged. A refractive index of 1.47 was used for the data treatment. Details of the procedure are given elsewhere.[4,6] The native oxide layer atop the silicon substrate leads to an overestimation of the film thickness by about 15 Å. X-ray reflectometry (XRR) studies were carried out on a Siemens D 5000 2-circles

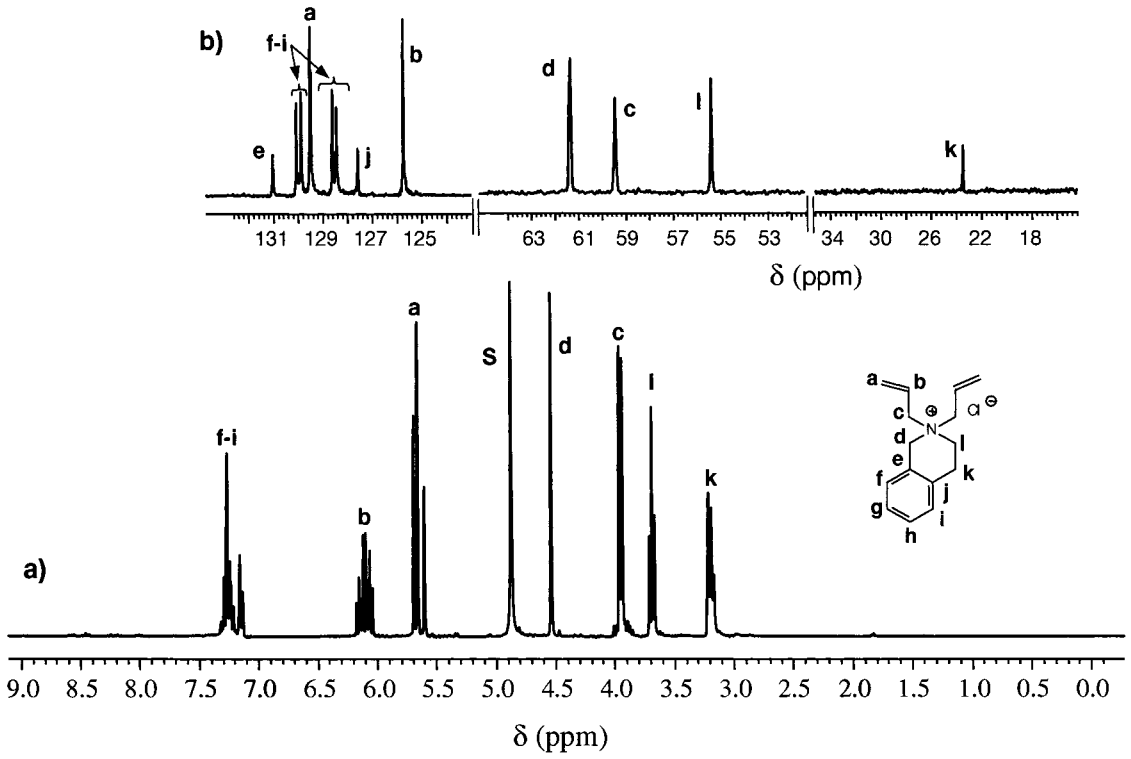

Figure 2. NMR spectra of monomer **3** in D_2O: top, ^{13}C NMR; bottom, ^1H NMR.

goniometer using Cu Kα radiation selected by a graphite secondary monochromator [(λ = 1.5418 Å) rotating anode operating at 40 kV and 300 mA]. The beam was collimated by slits adjustable with micrometer precision. A scintillation counter coupled to a pulse height analyzer was used as detector. A special automated alignment procedure allowed to position the sample within a few micrometers from the goniometer center. Additional information on the experimental set up can be found elsewhere.[4,6] The corrected intensities are reported as a function of K_{z_0}, the component perpendicular to the interface of the wave vector in the vacuum of the incident photons [i.e., $K_{z_0} = (2\pi/\lambda) \sin \theta$, where λ is the X-ray wavelength and θ is half the angle between the incident and reflected beams]. Intensities were multiplied by ${K_{z_0}}^4$ and plotted vs K_{z_0}. Then, Bragg peaks maxima were obtained by fitting plots with a Lorentzian function. Patterson functions were obtained by Fourier transformation as described elsewhere.[4] Topographic observations were performed on multilayered assemblies built up on silicon wafers without deposition of metal coating with a SEM FEG operated at 1 kV.

Synthesis of Monomers. *N*-Allyl-1,2,3,4-tetrahydroisoquinoline, 2. A 13.7 g (0.10 mol) sample of 1,2,3,4-tetrahydroisoquinoline (**1**) were added dropwise to 31.6 g (0.41 mol) of cold allyl chloride. The solution is stirred for 1 week at room temperature. Excess allyl chloride is evaporated and the residue dissolved in $CHCl_3$. The organic phase is washed three times with 50 mL of 1 M aqueous NaOH and evaporated. Purification by flash chromatography [silicagel; eluent, CH_2Cl_2/MeOH (90/10 v/v)]. TLC showed complete removal of starting materials. Yield: 8.81 g (49%) of yellow oil. Anal. Calcd for $C_{12}H_{15}N{\cdot}0.5H_2O$ (M_r = 173.26 + 0.5 × 18.02): C, 79.08; H, 8.30; N, 7.69; C/N = 10.3. Found: C, 79.38; H, 8.38; N, 7.39; C/N = 10.7. MS(FAB): m/z = 172.0. ^1H NMR (300 MHz, $CDCl_3$): δ = 7.35−7.10 [m, 4H, **Aryl**]; 6.20−6.05 [m, 1H, C=C**H**−C]; 5.50−5.30 [m, 2H, **H**$_2$C=C]; 3.78 [s, 2H, N−C**H**$_2$−Ph]. 3.30−3.36 [m, 2H, =C−C**H**$_2$−N]; 3.07 [t, 2H, N−C**H**$_2$−C]; 2.89 [t, 2H, C−C**H**$_2$−Ph].

***N*,*N*-Diallyl-1,2,3,4-tetrahydroisoquinolinium chloride (3).** As described for the alkylation of **1**, 12.3 g (0.071 mmol) of **2** are reacted with 76.5 g of allyl chloride (1.96 mmol). After evaporation of the excess allyl chloride, the crude product is precipitated in cold diethyl ether. The separated viscous oil is dissolved in 20 mL of water. The organic phase is washed with ether (50 mL), and then water is gently evaporated off. Final purification is achieved by filtration over basic alumina [solution eluent: CH_2Cl_2/MeOH (70/30 v/v)]. Yield: 17.1 g (61%) of reddish viscous oil. Anal. Calcd for $C_{15}H_{20}NCl{\cdot}H_2O$ (M_r = 249.78 + 18.02): C, 67.28; H, 8.28; N, 5.23; Cl, 13.24; C/N = 13.19. Found: C, 67.96; H, 7.97; N, 5.15; Cl, 13.59. C/N = 12.88. MS(FAB): m/z = (M − Cl^-)$^+$ = 214.1. ^1H NMR (300 MHz, CD_3OD): δ = 7.30−7.10 [m, 4H, **Aryl**]; 6.10 [m, 2H, C=C**H**−C]; 5.70−5.50 [m, 4H, **H**$_2$C=C]; 4.53 [s, 2H, N$^+$−C**H**$_2$−Ph]; 3.95 [d, 2H, C=C−C**H**$_2$]; 3.68 [t, 2H, N$^+$−C**H**$_2$−C]; 3.20−3.10 [m, 2H, C−C**H**$_2$−Ph]. ^{13}C NMR (75 MHz, CD_3OD): δ = 131.2 [(N$^+$)−C−**C**$_{\mathbf{Aryl}}$−]; 130.2−128.6 [=**C**$_{\mathbf{Aryl}}$H]; 129.6 [**C**$_{\mathbf{allyl}}$H$_2$=C]; 127.8 [C−C−**C**$_{\mathbf{Aryl}}$]; 125.9 [C=**C**$_{\mathbf{allyl}}$H]; 62.5 [(N$^+$)−**C**H$_2$−Ph]; 60.6 [(N$^+$)−**C**H$_2$−C=]; 56.6 [(N$^+$)−**C**H$_2$−C−]; 24.6 [C−**C**H$_2$−Ph].

Polymerization. Poly(*N*,*N*-diallyl tetrahydroisoquinolinium chloride) (4). The cationic monomer **3** was polymerized in 50 wt % aqueous solution, using 4 mol % of initiator relative to the monomer. After at least three freeze−thaw cycles, the reaction mixtures were either heated for 24 h at 60 °C using the free radical initiator VA086 or for 48 h at 70 °C using $K_2S_2O_8$. Polymers either were isolated by precipitation into acetone and/or were purified by dialysis in water for 3−5 days. Dialyzed polymers were recovered by lyophilization and dried overnight in vacuo at 40 °C. The absence of residual monomer was checked by ^1H NMR spectroscopy which show the complete disappearance of the signals of the diallylammonium moiety between 5 and 6 ppm. ^1H NMR [300 MHz, D_2O; see also Figure 3 for ^1H NMR performed in $(CD_3)_2SO$]: δ = 7.60−7.40 [two signals, 4H, **aryl H**]; 4.57 [broad, 2H, Ph−C**H**$_2$−(N$^+$)]; 3.74 [broad, 2H, Ph−C−C**H**$_2$−N$^+$]; 3.25 [broad, 2H, C−C−C**H**$_2$−(N$^+$)]; 2.64 [broad, −C−C**H**$_2$−Ph]; 1.80−0.90 [broad, C**H**$_2$ backbone]. Anal. Calcd for [$C_{15}H_{20}NCl{\cdot}5H_2O$, M = 339.86]$_n$: C, 53.01; H, 8.90; N, 4.12; O, 23.54; Cl, 10.43; C/N, 12.87. Found: C, 55.91; H, 7.62; N, 4.36; C/N = 12.82. Pinkish hygroscopic powder. ^{13}C NMR (75 MHz, CD_3OD): δ = 131.7, 131.5, 130.1, 129.9, 128.7, 128.4 [=**C**$_{\mathbf{Aryl}}$H]; 67.9 and 62.4 [(N$^+$)−**C**H$_2$−C]; 65.0 and 57.7 [(N$^+$)−**C**H$_2$−Ph]; 61.2 [(N$^+$)−**C**H$_2$−C-Ph]; 44.1, 39.8, 39.3, and 39.2 [(N$^+$)−**C**H$_2$−C]; 31.0 and 28.1 [(N$^+$)−C−**C**H$_2$−]; 26.2, 26.1, 25.3 [−**C**H$_2$−backbone]. The numerous signals derive from the complex stereochemistry of

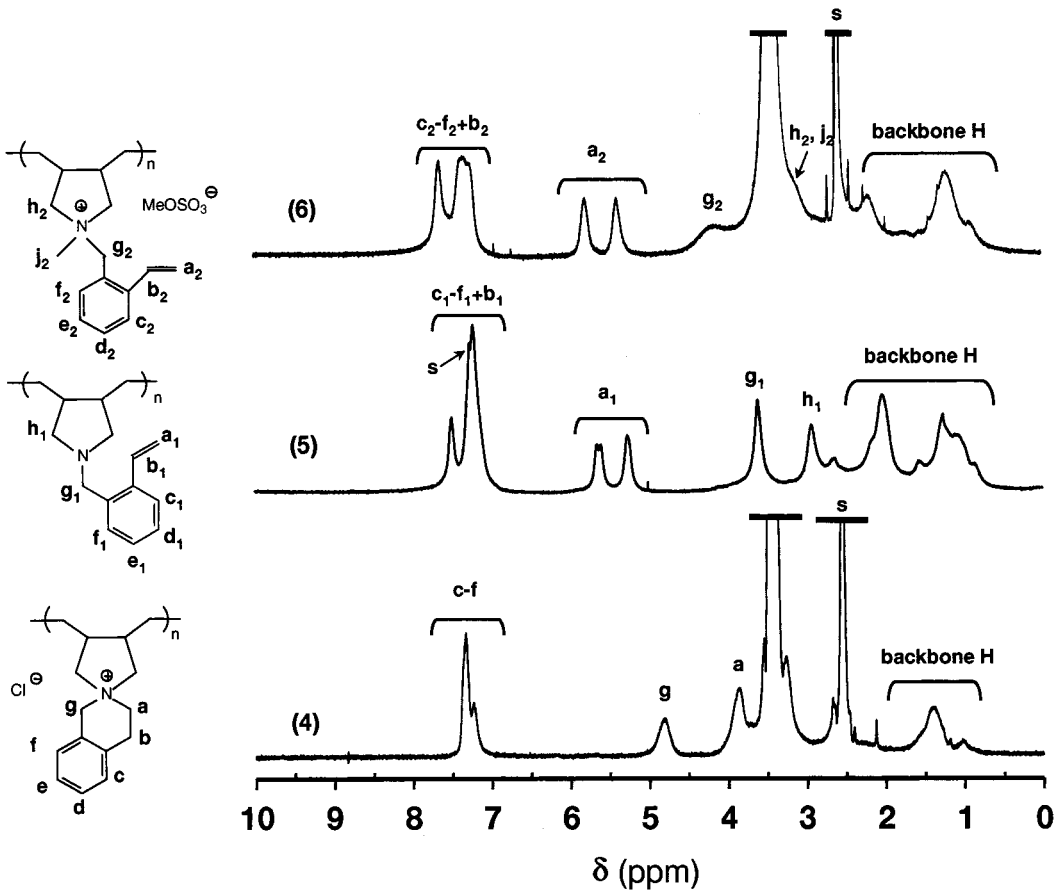

Figure 3. ^{1}H NMR spectra of polymers **4**−**6** in DMSO and $CDCl_3$ (from bottom to top).

the multiple substituted pyrrolidinium ring. FT-IR [KBr, selected bands (cm^{-1})]: 3066, 3029, 3005 (Ar−H, ortho-disubstituted; 2936, 2867 [CH, ν_{sym} and $\nu_{antisym}$]; 1119, [−O−SO_3−]; 756 [Ar−H, δ_{oop} ortho-disubstituted]; 619 [O−SO_3−]; 432 [Ar−H, ortho-disubstituted].

Chemical Modification of the Precursor Polymer via Hoffmann Elimination. Poly(*N*,*N*-diallyl-*N*-(2-vinylbenzyl)amine) (5). Under a dry argon atmosphere, 0.69 g (2.76 mmol) of polymer **4** in a 10 wt % homogeneous solution of DMF/*tert*-butyl alcohol 4/1 (v/v) were dissolved at 60 °C, and then allowed to cool to room temperature. After adding a small amount of quinone, 0.93 g (8.25 mmol) of potassium *tert*-butyl alcoholate were added to the mixture. The polymer which precipitates during the reaction is filtered off and thoroughly washed with water. Then, 0.35 g of **5** was recovered and dried in vacuo at room-temperature overnight. Yield: 59% in the form brownish powder. ^{1}H NMR (300 MHz, $CDCl_3$): δ = 7.49 and 7.21 [two broad signals, 5H, $\mathbf{H}_{Aryl}$ and C**H**=C]; 5.62 and 5.25 [two doublets, 2H, C$\mathbf{H}_2$=C]; 3.60 [s, 2H, N−C$\mathbf{H}_2$−Ph]. 2.92 [m, 2H, C−C$\mathbf{H}_2$−N]; 2.70−0.90 [broad signals, −C$\mathbf{H}_2$−, backbone]. ^{13}C NMR (75 MHz, $CDCl_3$): δ = 137.4, 129.8, 127.7, 127.4, 125.7 [=**C**H−$_{Aryl}$]; 134.9 [Ph−**C**H=]; 115.4 [Ph−C=**C**H_2]; 60.6 [N−**C**H_2−C=]; 58.6 [N−**C**H_2−Ph]; 40.5, 28.9 [N−C−**C**H_2 + −**C**H_2− (backbone)]. FT-IR [KBr, selected bands (cm^{-1})]: 3081, 3060, 3017, [CH=CH_2, ν]; 2922, 2855 [CH, ν_{sym} and $\nu_{antisym}$]; 1625 [C=C, ν]; 1413 [C=C, δ_s]; 1127 [−O−SO_3−]; 998 [CH=, δ_{oop}(trans wag)]; 910 [=CH_2, δ_{oop}(wag)]; 774, 761 [Ar−H, δ_{oop} ortho-disubstituted]; 619 [−O−SO_3−]; 424 [Ar−H, ortho-disubstituted].

Quaternization of the Polymer Amine Precursor. Poly(*N*,*N*-diallyl-*N*-methyl-*N*-(2-vinylbenzyl)ammonium) Methyl Sulfate (6). Polymer **5** [0.21 g (0.94 mmol)] was dissolved in DMF with 0.5 g (3.75 mmol) of dimethyl sulfate in the presence of a small amount of quinone. The homogeneous mixture is stirred overnight at room temperature. The quaternized polymer is repeatedly precipitated from a mixture of chloroform/ethanol [50/50 (v/v)] into cold ether, isolated, and dried at 40 °C in vacuo. Yield: 0.12 g (39%) of hygroscopic off-white powder. ^{1}H NMR [500 MHz, $(CD_3)_2SO$]: δ = 8.00−6.80 [3 signals, 5H, $\mathbf{H}_{Aryl}$ + C**H**=C]; 5.75 and 5.41 [2 signals, 2H, C$\mathbf{H}_2$=C]; 4.60−4.00 [broad, 2H, (N^+)−C$\mathbf{H}_3$]; 2.70−0.90 [broad, C$\mathbf{H}_2$, backbone]. FT-IR [KBr, selected bands (cm^{-1})]: 3081, 3062, 3025 [CH=CH_2, ν]; 2935, 2886 [CH, ν_{sym} and $\nu_{antisym}$]; 1626 [C=C, ν]; 1415 [C=C, δ_s]; 1121 [−O−SO_3−]; 996 [CH=, δ_{oop}(trans wag)]; 925 [=CH_2, δ_{oop}(wag)]; 778, 738 [Ar−H, δ_{oop} ortho-disubstituted]; 619 [−O−SO_3−]; 436 [Ar−H, ortho-disubstituted].

Results and Discussion

Synthesis of Monomers and Polymerization. Figure 1 schematizes the synthetic route leading to the tertiary amine **2** and to cationic monomer **3** as well as to the series of the new polymers **4**−**6**. The water-soluble monomer **3** is obtained by alkylating 1,2,3,4-tetrahydroisoquinoline (**1**) with allyl chloride in two steps under mild conditions (room temperature). The relatively poor yields of about 50% for both compounds **2** and **3** are attributed to the bulkiness of the amines. Typical ^{1}H NMR and ^{13}C NMR spectra of monomer **3** are illustrated in Figure 2. The characteristic signals of the protons and carbons of the allyl moiety are visible between 5.5 and 6.5 ppm and between 129.5 and 125.7 ppm respectively. The complex multiplet signal found at 3.2 ppm (see ^{1}H NMR in Figure 2) presumably results from a secondary coupling with the aromatic protons.

The polymerization of diallylammonium monomers is known for a number of particularities.[28,29] Despite the rather big substituents on the quaternary nitrogen atom, polymerization of **3** succeeded, however, with rather poor yields. Yields were typically lower than 10%

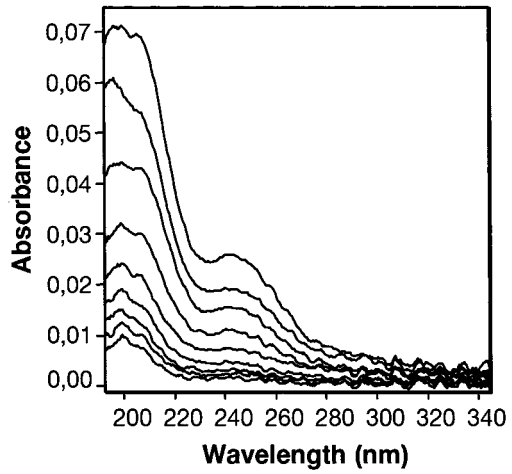

Figure 4. UV−vis absorbance spectra of assemblies $\{\mathbf{6},\boldsymbol{L}\}_n$ grown on quartz supports. From bottom to top: $n = 1, 2, 3, 4, 5, 7, 9, 13$.

(w/w) when the polymerization was initiated by the azo initiator VA086, whereas somewhat better yields of about 20%−25% were obtained when using $K_2S_2O_8$. Nevertheless, the presence of two bands centered around 1120 and 620 cm^{-1}, which are putatively attributed to vibrational modes of sulfate end groups, suggest relatively low molar masses for polycations **4**−**6** initiated with $K_2S_2O_8$. Polymer **4** is a polymeric spiro compound, and thus rather stiff compared to the parent polymer poly(dimethyldiallylammonium chloride), or to polymers **5** and **6**. On the basis of the molecular data of many other poly(dialkyldiallylammonium) salts,[24−26,28] we assume that the cyclopolymerization of **3** results in the kinetically favored formation of five-membered heterocycles, as proposed in Figures 1 and 3. In any case, the presence of four substituents on the heterocyclic ring gives rise to various forms of stereoisomerism, and therefore to complex NMR-spectra (Figure 3). Polymer **4** is converted into the reactive polymers **5** and **6** by Hoffmann elimination and subsequent methylation of the polymeric amine. The *o*-styrene substituent, which is newly formed on the quaternary nitrogen atom by this modification, enables cross-linking in a separate step by various mechanisms, such as 2 + 2 photocycloaddition, thermal and photopolymerization. The somewhat reduced reactivity of the 2-vinylbenzyl group compared to the 3- or 4-vinylbenzyl group facilitates the storage and the handling of the reactive polycations.

Miscellaneous Polymer Properties. Solubility. The hydrophobized polycation **4** is soluble at ambient temperature in a wide range of polar (aqueous and ethanol system) as well as weakly polar solvents ($CHCl_3$). The noncharged polymer intermediate **5** is not soluble in highly polar protic solvents such as water or methanol but is well-soluble in weakly polar ($CHCl_3$, CH_2Cl_2) and dipolar aprotic (DMF, DMSO) solvents. The reactive polycation **6** is insoluble in highly polar protic solvents such as water or ethanol, too, for both chloride or methyl sulfate as counterion. In contrast, **6** is well soluble at room temperature in amphiprotic alcohols (trifluoroethanol, tetrahydrofurfuryl alcohol) and aprotic dipolar solvents (DMF, DMSO) as well as in binary mixtures such as chloroform−methanol [∼50/50 (v/v)] or dioxane−water [∼50/50 (v/v)]. The observed limited solubility in classical protic solvents could result from the strong interactions between the aromatic fragments. This behavior is reminiscent of that exhibited by moderately

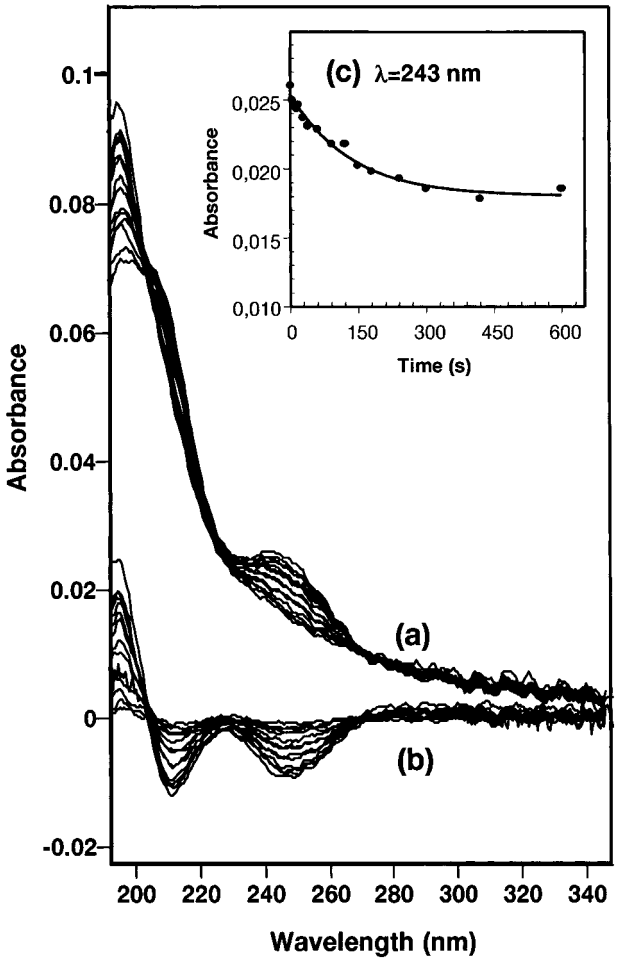

Figure 5. Cross-linking of multilayer films $\{\mathbf{6},\boldsymbol{L}\}_n$ followed by the change of the UV−vis spectra under irradiation by UV light of 254 nm. (a) Absorbance spectra [irradiation times (s)]: 0, 5, 15, 20, 30, 40, 60, 90, 120, 150, 180, 240, 300, 420, 600. (b) Difference spectra [irradiation times (s)]: 5, 10, 15, 20, 30, 50, 60, 90, 120, 150, 180, 240, 300, 420, 600. (c) Decrease of the absorbance at 243 nm upon irradiation.

hydrophobized charged polymers[30] for which binary mixtures of a strong apolar solvent with good solvation power for the apolar ring and a protic solvent capable of solvating the ionic moiety are required for dissolution.

Thermal Properties. Thermal stability of the new polymers was examined by thermogravimetry: The thermal cross-linking of polycation **5** that should occur at high temperatures is not accompanied by any significant change in the thermogravimetric curve (not shown). Heating leads to a slight and monotonic loss of weight from 80 until around 300 °C, where a major weight loss occurs in a one step. In the case of polymer **4**, two major decomposition steps were observed at about 280 and 400 °C, as well as two minor steps of weight loss detected below 200 °C. One of the steps is associated with the loss of water. Additional ^1H NMR (500 MHz, DMSO) and FTIR investigations up to 130 °C reveal slight changes in the spectra, but the underlying transformations could not be elucidated. In consequence, **4** was handled with great care when used at elevated temperatures. For this reason, the permanently charged polycation **4** was not exposed to temperatures higher than 175 °C when investigated by DSC. Thermograms (not shown) were essentially featureless. Successive scans exhibit only a broad endothermic peak that is attributed to a loss of residual bound water due to the

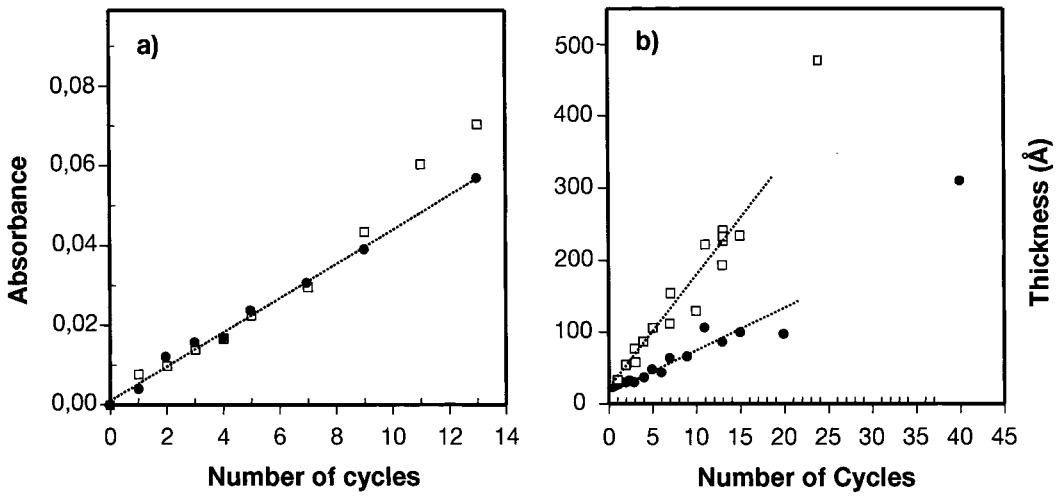

Figure 6. Growth of multilayers $\{\mathbf{6},\boldsymbol{L}\}_n$ of followed by (a) UV−vis absorbance at 243 nm and (b) ellipsometric thickness vs the number of deposition cycles: (●) = photo-cross-linked layer-by-layer; (□) = non-cross-linked samples (see text for more details).

strong hygroscopic character of **4,** as reflected by the data of elemental analysis.

Construction of Hybrid Multilayers. The ability of the system $\{\mathbf{6},\boldsymbol{L}\}_n$ to form films on quartz supports from DMSO based system was verified by UV−vis spectroscopy. Figure 4 shows the absorbance spectra of the un-cross-linked multilayers as a function of the number of deposition cycles. Continuous film deposition is confirmed by the monotonic increase in intensity of the bands located at 205 and 243 nm corresponding to $\pi \rightarrow \pi^*$ transitions of the styrene fragment. This moiety is photoreactive when exposed to UV light. Figure 5 shows the change in the absorbance spectra of a film $\{\mathbf{6},\boldsymbol{L}\}_{13}$ exposed to different cumulative times of UV irradiation. Most notably, the peak at 243 nm loses intensity and finally disappears. Further, the band at 205 nm changes its shape. The difference spectra shown in Figure 5 illustrate even more clearly these changes. The existence of two isosbestic points suggests a rather clean photoreaction, that could be a 2 + 2 photocycloaddition or a photopolymerization. Either of them will lead to cross-linked multilayer films. Exposure times of about 10 min are sufficient to achieve virtually full conversion of the reactive group (Figure 5c). Preliminary experiments illustrate that photo-cross-linking improves the stability of the assemblies to powerful solvents, such as a saturated solution of $CaCl_2$ in DMF, that removes, e.g., about 30% of the total thickness of the non-cross-linked film after 5 min of exposure at 50 °C.

The variation of the absorbance at 243 nm as a function of the number of deposition cycles is presented in Figure 6a. As reported elsewhere, growth of ESA films from hydrophobized polyelectrolytes with other polyelectrolytes including inorganic clays[6] on hydrophilic substrates does not pose any particular problem. However, growth is no longer linear from six to seven deposition cycles on. Such a behavior may have several reasons, e.g., restructuration of the film outer layers during deposition, increasing roughness of the films surface, deposition of patches instead of continuous smooth layers, etc. Interestingly, more regular growth is observed when the assemblies are cross-linked after each deposition step of the polycation, showing the beneficial effect of cross-linking on the self-assembly process. This finding is in good agreement with previous results for purely organic polyelectrolyte multilayers.[18a]

Table 1. Ellipsometric and X-ray Reflectivity Data of the Crosslinked and Not Crosslinked $\{6,L\}_n$ Multilayers

$\{\boldsymbol{6},\boldsymbol{L}\}_n$ films	av thickness increment/cycle (Å/cycle ± 1 Å)[c]	repeat dist (Å ± 0.5 Å)[b]	av thickness (Å ± 5 Å)[a]	
un-cross-linked	19	16.3 (n = 7)	155[b] (n = 7)	138[c]
during		16.1 (n = 10)	222[b] (n = 11)	211[c]
buildup		15.8 (n = 15)	242[b] (n = 13)	226[c]
cross-linked	5	17.4 (n = 11)		
during		16.1 (n = 13)		
buildup		15.9 (n = 15)		
		14.8 (n = 20)		
		14.5 (n = 40)		

[a] From ellipsometric measurements. [b] From X-ray reflectometry measurements. [c] Immediately after cross-linking of multilayer film by ellipsometry.

Similar experiments performed on silicon wafers allowed to follow the evolution of the average film thickness by ellipsometry. Although continuous film growth is evident from Figure 6b, the thickness increment per number of adsorption cycle is no longer regular from seven cycles on for un-cross-linked multilayers, in good agreement with the UV−vis measurements. Deviation from linear growth occurs only for a larger number of deposition cycles (>10) for cross-linked layers, which is again in agreement with the UV−vis studies.

Non-cross-linked multilayers $\{\mathbf{6},\boldsymbol{L}\}_n$ grow much more rapidly than the cross-linked ones, as demonstrated by the average thickness increments per deposition cycle listed in Table 1. For cross-linked multilayers, the low increment that is much smaller than the thickness of Laponite platelets (9 Å) is striking, and a partial desorption following cross-linking cannot be rigorously excluded for this system. In any case, these observations suggest that layer-by-layer film growth for cross-linked or non-cross-linked $\{\mathbf{6},\boldsymbol{L}\}_n$ hybrid assemblies, does not proceed simply by deposition of coherent stratas of polyelectrolyte or clay sheets but instead implies the successive filling of the incomplete layers previously deposited. In other words, for this particular system, film growth not only takes place in the vertical direction as usually assumed but also requires increased filling of the adsorbed layers in the lateral direction, as already invoked recently for other hybrid systems.[31] This conclusion is supported by SEM micrographs as shown in

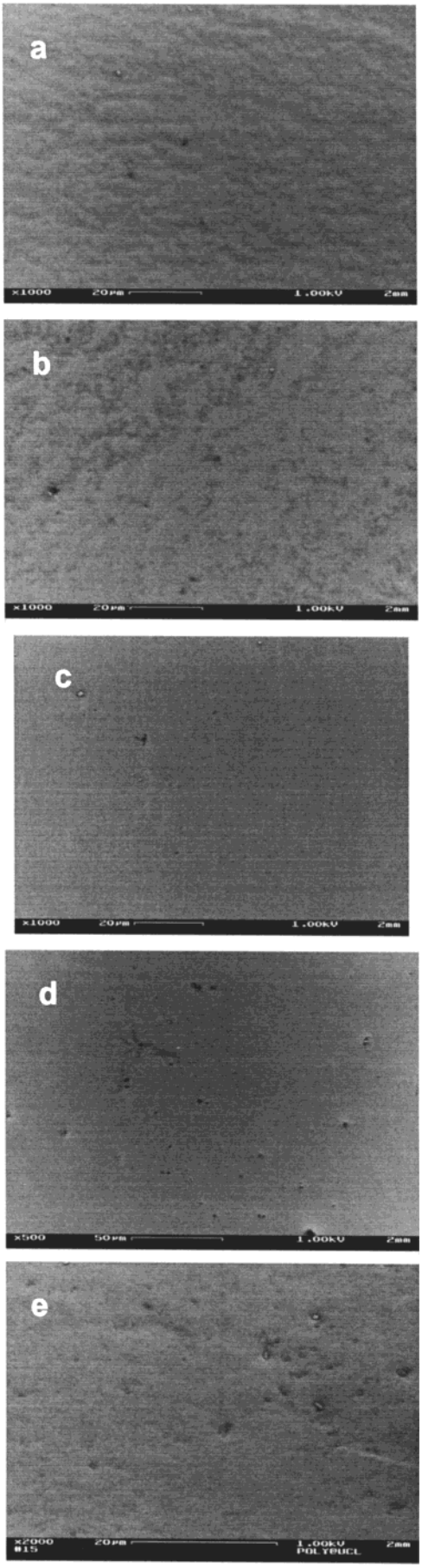

Figure 7. SEM images of (a) non-cross-linked $\{\mathbf{6},\boldsymbol{L}\}_1$ assembly (×1000) and (b) $\{\mathbf{6},\boldsymbol{L}\}_n$ cross-linked assemblies with (c) $n = 2$ (×1000), (d) $n = 3$ (×500), and (e) $n = 10$ (×2000).

Figure 7, showing a morphology with holes distributed all over the surface.

X-ray reflectograms obtained from cross-linked and non-cross-linked assemblies are given in Figure 8. The occurrence of a broad Bragg diffraction peak, similar in shape in both cases, proves that the assemblies dispose to some degree of an internal structure. This is also clearly visible from the computed Patterson functions by the presence of two oscillations near zero interdistance (Figure 8). However, the dramatic damping of the Patterson function with distance illustrates quite well the limited extent of the order, correlations extending only approximately to three layers (i.e., 40−50 Å), as discussed elsewhere.[6]

Interestingly, the internal structure of the cross-linked assemblies is subject to certain modifications during the deposition process. This is shown by slight variations in the position and in the intensity of the Bragg peak. An unambiguous explanation cannot be provided for explaining the shift of the Bragg peak to higher angles as depicted in Figure 9. As a partial degradation of polycation **6** under UV light conditions cannot not be completely excluded, the elimination of a certain amount of polyelectrolyte in the subsequent immersions in DMSO could contribute to decrease the basal spacing of the Laponite strata (see Table 1). For instance, the photodecomposition of benzylammonium salts by deep UV irradiation is well documented.[32] However, such an explanation appears difficult to justify considering the absolute growth of the assemblies. Alternatively, interpenetration of successive layers followed by cross-linking may result in the progressive buildup of retraction (entropic) forces, which would cause some water expulsion with an subsequent shrinkage of the Bragg distance. However, overall, cross-linking does not affect strongly the structural characteristics of the multilayers, which will be analyzed in details elsewhere.

In addition to the Bragg peaks, the position and the number of the Kiessig fringes that are typically displayed in the small angle region of the X-ray reflectograms provide information on the thickness and the roughness of the films. In marked contrast to the absence of Kiessig fringes in the scattering profiles of un-cross-linked assemblies $\{\mathbf{6},\boldsymbol{L}\}_n$ (see Figure 8a), two fringes are observed for cross-linked samples, indicating that the photoreaction is beneficial for the films' smoothness. This is also exemplified by the SEM images shown in Figure 7. A similar behavior was already reported for LBL films after microwave irradiation.[33] These findings could be explained such that less reorganization during the film growth should occur in the underlying layers in cross-linked samples and that the cross-linking of the uppermost layer hampers the intermingling of heterospecies during the tiling process. Also, due to the better surface coverage, it is expected that the same amount of polymers is adsorbed in each cycle leading to more defined interfaces. Finally, cross-linking will probably reduce the detrimental effects on surface morphology arising from the dipping of the multilayers in solution of successively good and poor solvent of **6**.

Alternatively to a cross-linking after each deposition of a reactive polycation layer, multilayer films can be cross-linked after the completed buildup. Ellipsometry was applied to investigate the effect of the cross-linking reaction on the films' thickness, performed at the end of the deposition process. After 10 min of exposure to

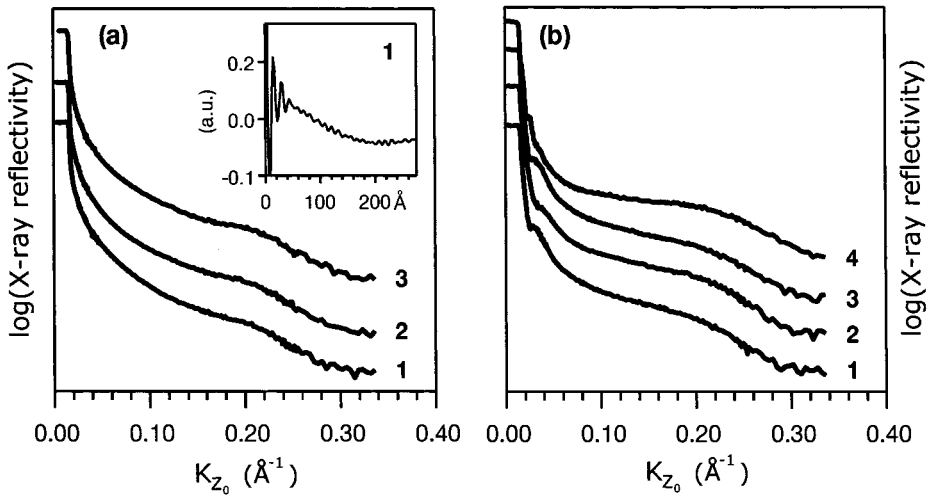

Figure 8. X-ray reflectograms of multilayers $\{\mathbf{6},\boldsymbol{L}\}_n$ grown on Si-wafers [100]: (a) non-cross-linked [(1) $n = 7$ cycles; (2) $n = 11$ cycles; (3) $n = 15$ cycle]; (b) cross-linked [(1) $n = 13$ cycles; (2) $n = 15$ cycles; (3) $n = 20$ cycles; (4) $n = 40$ cycles]. Inset: Patterson function of $\{\mathbf{6},\boldsymbol{L}\}_{15}$ assemblies.

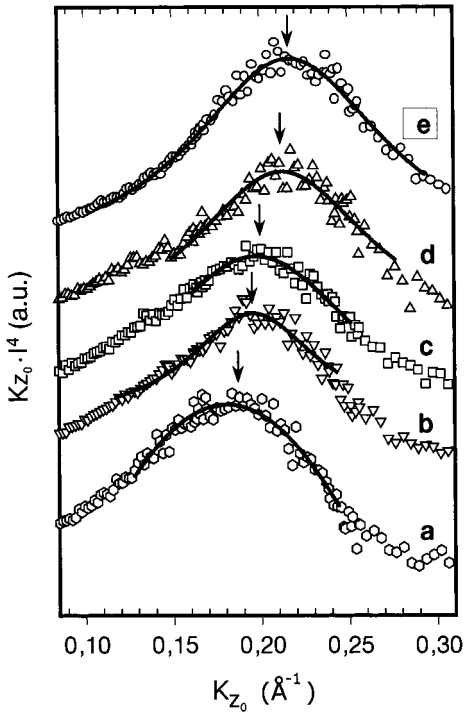

Figure 9. X-ray reflectivity of cross-linked multilayers $\{\mathbf{6},\boldsymbol{L}\}_n$ grown on Si wafers [100], with intensities multiplied by $K_{Z_0}{}^4$: (a) $n = 11$ cycles; (b) $n = 13$ cycles; (c) $n = 15$ cycles; (d) $n = 20$ cycles; (e) $n = 40$ cycles. Intensities are normalized and curves displaced vertically for clarity.

UV light, the impact of the cross-linking reaction is perceptible with a decrease in the samples thickness of around 5−10%. The decrease is slightly higher than the experimental imprecision. The observed shrinkage seems too big to be only attributed to a volume contraction induced by the cross-linking step as such. As discussed above, it might be caused by a partial photodecomposition of the benzylammonium moiety (though not probable), too, or by a reduced hydration of the cross-linked layers. In any case, it is clear that stabilized thicker hybrid films (compared to the step-by-step photo-cross-linking) can be obtained in two steps, by completely separating film construction and cross-linking.

Conclusions

A new cross-linkable poly(diallylammonium) salt was synthesized in an attempt to stabilize electrostatically assembled hybrid multilayers. The reactive polycation can be self-assembled with complementary charged, delaminated clay platelets, such as the synthetic hectorite Laponite. Only short time exposure to UV light is required to cross-link the films. The photoreaction reduces the films' roughness and promotes more regular growth. From a practical of view, this approach may offer additional benefits, such as improving the barrier functionality of the inorganic layers[12] as well as the control of the permeability between pure organic sublayers.

Acknowledgment. The authors thank A. Moussa and A. Pallandre for the help given for the fabrication of the multilayers and SEM microscopy. K. Glinel is acknowledged for stimulating discussions on hybrid multilayers, and the help provided for the X-ray reflectometry measurements. Discussions with J.-L. Habib-Jiwan were highly appreciated. Financial support was provided by the Belgian National Fund for Scientific Research, and by the DG Recherche Scientifique of the French Community of Belgium (Action de Recherche Concertée, convention 00/05-261).

References and Notes

(1) (a) Decher, G. *Science* **1997**, *277*, 1232. (b) Decher, G. In *The Polymer Materials Encyclopedia: Synthesis, Properties and Applications*; Salamone, J. C., Ed.; CRC Press: Boca Raton, FL, 1996; p 4540. (c) Decher, G. *Comprehensive Supramolecular Chemistry (Templating, Self-Assembly and Self-Organization)*; Oxford: Oxford, England, 1996, Vol. 9, p 507.

(2) See review articles: (a) Bertrand, P.; Jonas, A.; Laschewsky, A.; Legras, R. *Macromol. Rapid Commun.* **2000**, *21*, 319. (b) Arys, X.; Jonas, A. M.; Laschewsky, A.; Legras, R. *Supramolecular Polymers*; Cifferi, A., Ed. Marcel Dekker: New York, 2000; p 505.

(3) (a) Laschewsky, A.; Mayer, B.; Wischerhoff, E.; Arys, X.; Jonas, A. *Ber. Bunsen-Ges. Phys. Chem.* **1996**, *100*, 1033. (b) Fischer, P.; Laschewsky, A.; Wischerhoff, E.; Arys, X.; Jonas, A.; Legras, R. *Macromol. Symp.* **1999**, *137*, 1.

(4) (a) Arys, X.; Laschewsky, A.; Jonas, A. M. *Macromolecules* **2001**, *34*, 3318. (b) Bollinne, C.; Stone, V. W.; Carlier, V.; Jonas, A. M. *Macromolecules*, **1999**, *32*, 4719.

(5) Lvov, Y.; Decher, G. *Cryst. Rep.* **1994**, *4*, 628.

(6) Glinel, K.; Laschewsky, A.; Jonas, A. M. *Macromolecules* **2001**, *34*, 5267.

(7) (a) Kim, H. N.; Keller; S. W.; Mallouk, T. E.; Schmitt, J.; Decher, G. *Chem. Mater.* **1997**, *9*, 1414. (b) Struth, B.; Eckle, M.; Decher, G.; Oeser, R.; Simon, P.; Schubert, D. W.; Schmitt, J. *Eur. Phys. J. E* **2001** *6*, 351.
(8) Kotov, N. A.; Dékány, I.; Fendler, J. H. *Adv. Mater.*. **1996**, *8*, 637.
(9) (a) Kleinfeld, E. R.; Fergusson, G. S. *Science* **1994**, *265*, 370; (b) *Chem. Mater.* **1995**, *7*, 2327; (c) *Chem. Mater.* **1996**, *8*, 1575.
(10) Glinel, K.; Jonas, A. M.; Laschewsky, A.; Vuillaume, P. Y. Strategies to Internally Structured Polyelectrolyte Multilayers. In *Thin Films: Polyelectrolyte Multilayers and Related Multicomposites*; Decher, G., Schlenoff, J., Eds.; J. Wiley-VCH: New York, in press.
(11) Glinel, K.; Laschewsky, A.; Jonas, A. M. To be submitted.
(12) Eckle, M.; Decher, G. *Nano Lett.* **2001**, *1*, 45.
(13) (a) Lagaly, G. Smectic Clays as Ionic Macromolecules. In *Developments in Ionic Polymers*; Wilson, A. D., Posser, H. T., Eds.; Applied Science Publishers: London, 1986; p 77. (b) *Appl. Clay Sci.* **1999**, *15*, 1.
(14) Mathauer, K.; Schmidt, A.; Knoll, W.; Wegner, G. *Macromolecules* **1995**, *28*, 1214.
(15) Laschewsky, A.; Ringsdorf, H. *Macromolecules* **1988**, *21*, 1936.
(16) (a) Cemel, A.; Fort, T.; Lando, *J. Polym. Sci., Polym. Chem. Ed.* **1972**, A*10* 2061. (b) Ackermann, J. B.; Naegele, D.; Ringsdorf, H. *Makromol. Chem.* **1974**, *175*, 699. (c) Tieke, B.; Graf, H. J.; Wegner, G.; Naegele, D.; Ringsdorf, H.; Banerjie, A.; Day, D.; Lando, J. B. *Colloid Polym. Sci.* **1977**, *255*, 521. (d) Laschewsky, A.; Ringsdorf, H.; Schmidt, G. *Thin Solid Films.* **1985**, *134*, 153.
(17) Nakanishi, F.; Nagasawa, J.; Tamada, K.; Yoshida, M.; Akiyama, H.; Gong, Y. K.; Abe, K. *Am. Chem. Soc., Polym. Prepr.* **1998**, *39* (1), 355.
(18) (a) Laschewsky, A.; Wischerhoff, E.; Bertrand, P.; Delcorte, A. *Macromol. Chem. Phys.* **1997**, *198*, 3239. (b) Vuillaume, P. Y.; Jonas, A. M.; Laschewsky, A. To be submitted.
(19) Rouse, J. H.; MacNeill, B. A.l Ferguson, G. S. *Chem. Mater.* **2000**, *12*, 2502.
(20) (a) Brynda, E.; Houska, M. *J. Colloid Interface Sci.* **1996**, *183*, 18. (b) Brynda, E.; Houska, M. *Macromol. Rapid Commun.* **1998**, *19*, 173. (b) Kim, H.; Urban, M. W. *Langmuir* **1998**, *14*, 7235. (c) Leporatti, S.; Voigt, A.; Mitlohner, R.; Sukhorukov, G.; Donath, E.; Möhwald, H. *Langmuir* **2000**, *16*, 4059. (d) Sirkar, K.; Revzin, A.; Pishko, M. V. *Anal. Chem.* **2000**, *72*, 2930. (e) Voigt, A.; Buske, N.; Sukhorukov, G. B.; Antipov, A. A.; Leporatti, S.; Lichtenfeld, H.; Baumler, H.; Donath, E.; Möhwald, H. *J. Magn. Magn. Mater.* **2001**, *225*, 59.
(21) (a) Harris, J. J.; DeRose, P. M.; Bruening, M. L. *J. Am. Chem. Soc.* **1999**, *121*, 1978. (b) Ichinose, I.; Muzuki, S.; Ohno, S.; Shiraishi, H.; Kunitake, T. *Polym. J. Jpn.* **1999**, *31*, 1065. (c) Mendelsohn, J. D.; Barrett, C. J.; Chan, V. V.; Pal, A. J.; Mayes, A. M.; Rubner, M. F. *Langmuir* **2000**, *16*, 5017. (d) Dai, J.; Jensen, A. W.; Mohanty, D. K.; Erndt, J.; Bruening, M. L. *Langmuir* **2001**, *17*, 931. (e) Stair, J. L.; Harris, J. J.; Bruening, M. L. *Chem. Mater.* **2001**, *13*, 2641. (f) Sullivan, D. M.; Bruening, M. L. *J. Am. Chem. Soc.* **2001**, *123*, 11805. (g) Jiang, X. P.; Hammond, P. T. *Adv. Mater.* **2001**, *13*, 1669.
(22) (a) Chen, J.; Huang, L.; Ying, L.; Lin, G.; Zhao, X.; Cao, W. *Langmuir* **1999**, *15*, 7208. (b) Cao, W. X.; Sun, J.; Wang, Z.; Wu, L.; Zhang, X.; Shen, J.; Gao, S.; Chi, L.; Fuchs, H. *Macromol. Chem. Phys.* **2001**, *202*, 967. (c) Zhao, X. Sh.; Cao, W. X.; Li, M. Q.; Wei, Y. *Macromol. Rapid Commun.* **2001**, *22*, 583. (d) Zhang, Y.; Cao, W. X. *Langmuir* **2001**, *17*, 5021. (e) Zhang, Y.; Cao, W. X. *Macromol. Rapid Commun.* **2001**, *22*, 842. (f) Yang, B.; Shen, J.; Yu, G.; Cao, W. X. *Macromol. Chem. Phys.* **2001**, *202*, 2174. (g) Luo, H.; Chen, J. Y.; Luo, G. B.; Chen, Y. N.; Cao, W. X. *J. Mater. Chem.* **2001**, *11*, 419.
(23) Yang, Y. J.; Engberts, J. F. B. N. *J. Org. Chem.* **1991**, *56*, 4300.
(24) (a) Ali, S. A.; Rasheed, A.; Wazeer, M. I. M. *Polymer* **1999**, *40*, 2439. (b) Ali, S. A.; Rasheed, A. *Polymer* **1999**, *40*, 6849. (c) Ali, S. A.; Saeed, M. T. *Polymer* **2001**, *42*, 2785.
(25) (a) Favresse, P.; Laschewsky, A. *Macromol. Chem. Phys.* **1999,** *200*, 887. (b) Favresse, P.; Laschewsky, A. *Polymer* **2001**, *42*, 2755.
(26) De Vynck, V.; Goethals, E. J. *Macromol. Rap. Commun.* **1997**, *18*, 149.
(27) Kleim, R.; Kuntzler, L.; El Ghemmaz, A. *J. Opt. Soc. Am. A* **1994**, *11*, 2550.
(28) Hahn, M.; Jaeger, W. *Angew. Makromol. Chem.* **1992**, *198*, 165.
(29) Wandrey, C.; Hernández-Barajas, J.; Hunkeler, D. *Adv. Polym. Sci.* **1999**, *145*, 134.
(30) Laschewsky, A.; Zerbe, I. *Polymer* **1991**, *32*, 2070. (b) Köberle, P.; Laschewsky, A. *Macromolecules* **1994**, *27*, 2165.
(31) Ostrander, J. W.; Mamedov, A. A.; Kotov, N. A. *J. Am. Chem. Soc.* **2001**, *123*, 1101.
(32) Arndt, T.; Häussling, L.; Ringsdorf, H.; Wegner, G. *Adv. Mater.* **1991**, *3*, 58.
(33) Correa Duarte, M. A.; Giersig, M.; Kotov, N. A.; Liz-Marzán, L. M. *Langmuir* **1998**, *14*, 6430.

MA012095A